



Contents lists available at ScienceDirect

Bioorganic & Medicinal Chemistry Letters

journal homepage: www.elsevier.com/locate/bmcl

Optimization of a pyrazole hit from FBDD into a novel series of indazoles as ketohexokinase inhibitors

Xuqing Zhang*, Fengbing Song, Gee-Hong Kuo, Amy Xiang, Alan C. Gibbs, Marta C. Abad, Weimei Sun, Lawrence C. Kuo, Zhihua Sui

Johnson & Johnson Pharmaceutical Research and Development, Welsh & McKean Roads, PO Box 776, Spring House, PA 19477, United States

ARTICLE INFO

Article history:

Received 2 May 2011

Revised 14 June 2011

Accepted 15 June 2011

Available online 29 June 2011

Keywords:

FBDD (fragment based drug discovery)

KHK (ketohexokinase)

Pyrazole

Indazole

ABSTRACT

A series of indazoles have been discovered as KHK inhibitors from a pyrazole hit identified through fragment-based drug discovery (FBDD). The optimization process guided by both X-ray crystallography and solution activity resulted in lead-like compounds with good pharmaceutical properties.

© 2011 Elsevier Ltd. All rights reserved.

Ketohexokinase (KHK, also known as fructokinase) catalyzes, with adenosine triphosphate (ATP) and a potassium ion (K^+), the conversion of the furanose form of D-fructose to fructose-1-phosphate.¹ It initiates the intracellular catabolism of a large proportion of dietary carbohydrate and is an important regulator of hepatic glucose metabolism.² Due to its role in dietary fructose metabolism, inhibition of KHK would suppress carbon supply for fatty acid and very low density lipoprotein synthesis. Hence, modulation of KHK will help relieve some metabolic syndromes such as obesity, hypertriglyceridemia, insulin resistance and hypertension, which makes KHK an important target in drug discovery.³

Recently, a novel series of pyrimidinopyrimidines have been discovered by using a combination of high-throughput screening (HTS) and structure-based drug design (SBDD).⁴ Along with HTS approach, we also described a different approach for lead generation of KHK inhibitors through a FBDD protocol.⁵ The entire process includes X-ray crystallographic screening of three stages of iterative design and synthesis of fragment libraries. We have described the discovery of unique and structurally diverse hits through this pathway. Herein we focus on a medicinal chemistry approach to drive one hit into lead-like structures. Unlike the early libraries solely guided by electron density information from X-ray crystallography, the follow-up compounds were evaluated in a KHK-mediated enzymatic assay. Selected compounds were ad-

vanced into lead optimization or late lead generation according to their bio-activity, pharmacokinetic and selectivity profiles.

Fragment evolution has been by far the most successful method of fragment optimization.^{6–9} When allied with a high degree of structural information such as X-ray crystallography, it gives medicinal chemists valuable tools in the validation and subsequent optimization of a hit. Pyrazole **1** (Fig. 1) was identified as a hit binding to the ATP binding site of KHK by X-ray crystallographic screening of the fragment libraries. Without KHK enzyme activity tested, fragment **1** was optimized in the follow-up chemistry. Figure 1 illustrates the combination of fragment fusion and evolution of pyrazole **1** to yield indazole **2**. Evidence supporting incorporation of an indazole core was an intra-molecular H-bonding between the 4-carboxamide and 5-amine functional groups of pyrazole **1**, as revealed by X-ray crystallography, molecular mechanics and virtual docking experiments. Furthermore, as indicated by X-ray crystallography, these two functional groups

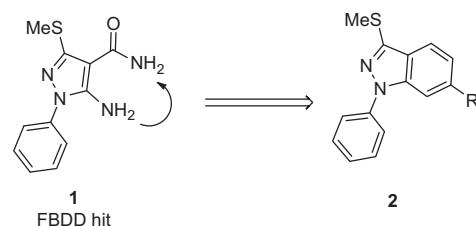


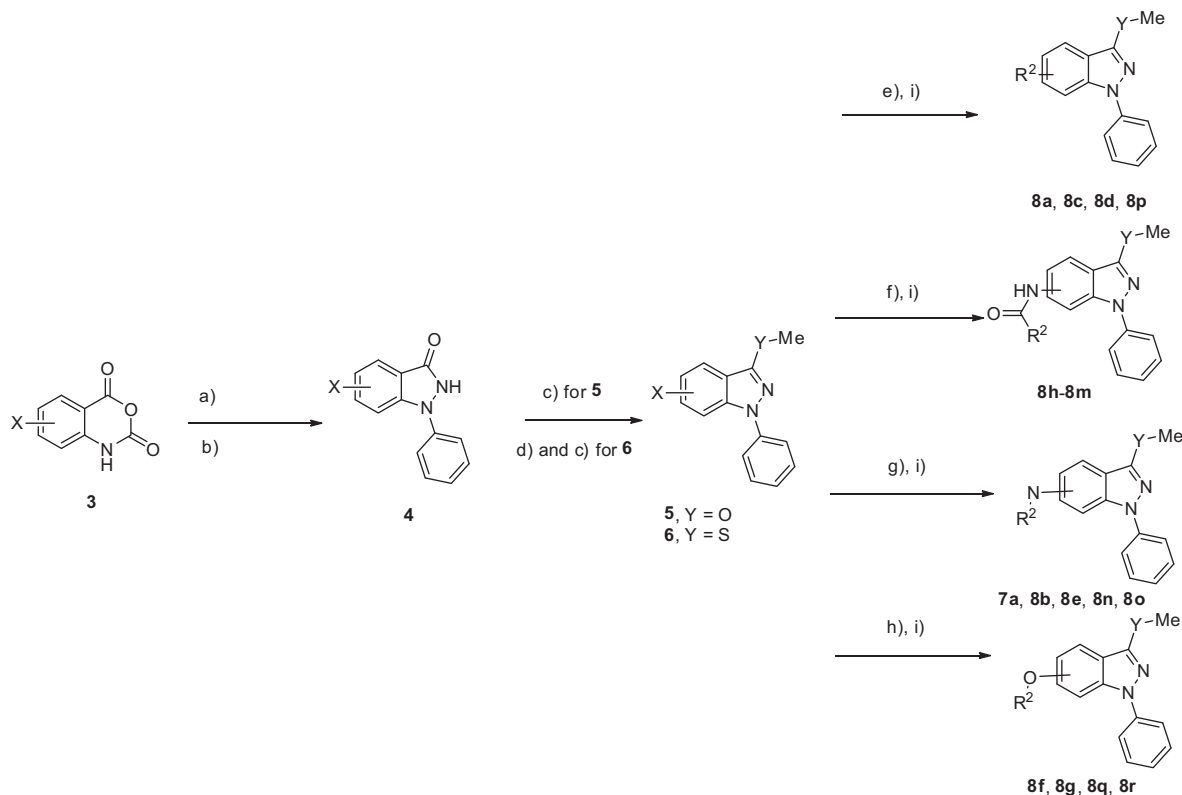
Figure 1. From pyrazole to indazole.

* Corresponding author. Tel.: +1 215 488 7866.

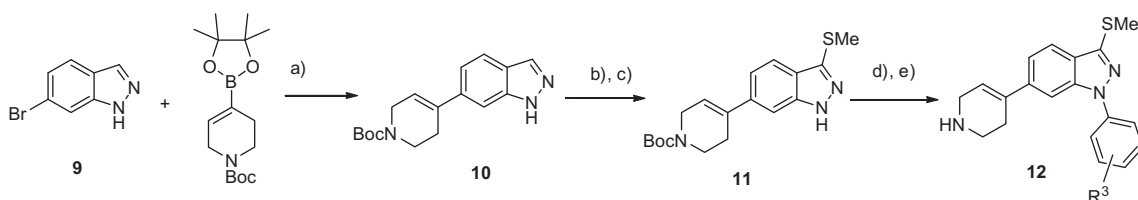
E-mail address: xzhang5@its.jnj.com (X. Zhang).

did not engage in obvious H-bonding with the protein. Thus, 6,5-fused systems such as an indazole core became one of the logical designs provided that indazole could be tolerated in the binding pocket. This strategy was also supported by the observation that some phenyl fragments, while not hits from X-ray screening, overlapped well with the amine/carboxamide moieties of pyrazole **1**. From medicinal chemistry perspective, indazole template **2** allowed further substitution (R^2) on the phenyl ring to extend into

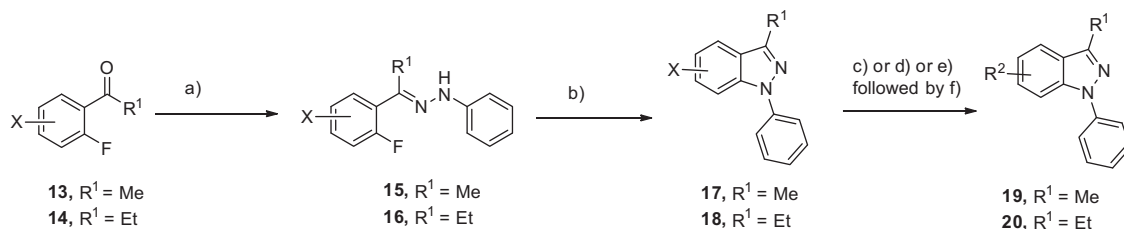
the binding site. Substituted indazole analogs could be easily synthesized and quickly derivatized. Thus, indazole **2** was considered as a major chemotype in the follow-up chemistry. Docking of indazole **2** with a X-ray crystal structure of pyrazole **1** revealed that **2** overlapped closely with **1** and was $\sim 6\text{--}7\text{ \AA}$ from the Asp27 carboxylate of the *b* subunit that forms the KHK dimer (Asp27B). A series of indazole analogs were synthesized and evaluated as KHK inhibitors. Considering the acidic nature of Asp27B, we designed



Scheme 1. Reagents and conditions: (a) PhNHNH₂, DIPEA, rt; (b) NaNO₂, HCl; (c) Cs₂CO₃, MeI; (d) P₂S₅, xylene, 130 °C; (e) for **8c, 8d, 8p**, X = Br: Pd(PPh₃)₄, Boc-R²-B(OH)₂, Na₂CO₃; H₂, Pd/C (for **8a**); (f) for **8h–m**, X = NO₂: H₂, Pd/C; HATU, COOH-R²-Boc; (g) for **7a, 8b, 8e, 8n, 8o**, X = Br: Pd(OAc)₂, Cs₂CO₃, BINAP, Boc-R²NH, toluene, reflux; (h) for **8f, 8g, 8q, 8r**, X = OMe: BBr₃; Cs₂CO₃, TSO-R²-Boc; and (i) HCl.



Scheme 2. Reagents and conditions: for **12a–g** (a) Pd(PPh₃)₄, Na₂CO₃; (b) KOH, I₂; (c) NaSMe, t-Bu-ONa, Pd(OAc)₂, Josiphos; (d) Boc-R³-Ph-B(OH)₂, Cu(OAc)₂; and (e) HCl; for **12g**, Fe, HOAc (R³ from NO₂ to NH₂).



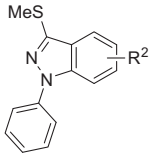
Scheme 3. Reagents and conditions: (a) PhNHNH₂, TSA; (b) K₂CO₃, DMF, 100 °C; (c) for **19a–b, 20a–h**, X = Br: Pd(OAc)₂, Cs₂CO₃, BINAP, Boc-R²-NH, toluene, reflux; (d) for **20i**, X = Br: Pd(PPh₃)₄, Boc-R²-B(OH)₂, Na₂CO₃; (e) for **20k**, X = NO₂: H₂, Pd/C; HATU, Boc-R²-COOH; for **20j**, HCl (gas), MeOH followed by NH₄OAc; and (f) HCl.

the indazoles containing basic amino groups to target potentially favorable ionic ligand–protein interactions. The size, length, rigidity and geometry of the R² group were modified for favorable interactions with negatively charged Asp27B.

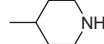
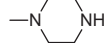
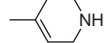
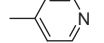
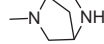
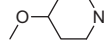
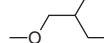
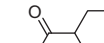
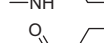
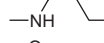
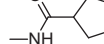
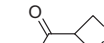
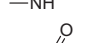
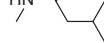
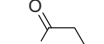
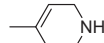
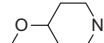
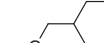
The general synthetic route to indazole analogs **7** and **8** is shown in Scheme 1. Phenylhydrazine was reacted with substituted 1H-benzo[d][1,3]oxazine-2,4-diones **3** either commercially available or prepared according to the literatures followed by intramolecular cyclization via diazotization to provide 1-phenyl-1H-indazol-3(2H)-ones **4** in 35–52% yield. Indazolones **4** were methylated with cesium carbonate and methyl iodide to afford 3-methoxy-1-phenyl-1H-indazoles **5** in 65–71% yield. Indazolones **4** were converted into thio-indazolones by treatment with P₂S₅ in toluene followed by thio-alkylations with methyl iodide to afford the corresponding 3-(methylthio)-1-phenyl-1H-indazoles **6** in 28–40% yield. Compounds **5** and **6** were functionalized at 6- or 7-position (R²) of indazole core via Suzuki coupling, Buchwald amination, amide coupling or displacement strategies. Bromo-indazole **6** was coupled with aryl boronic acid under standard Suzuki conditions, followed by de-protection of *N*-Boc group to afford **8c**, **8d** and **8p**. Compound **8a** was obtained by hydrogenation of **8c**. Bromo-indazole **6** was also converted into **7a**, **8b**, **8e**, **8n** and **8o** through Buchwald amination followed by de-protection of the *N*-Boc group. For synthesis of the amide side chain on the indazole core, nitro-substituted indazole **6** was reduced under hydrogenation to give an amino indazole intermediate, which was then coupled with carboxylic acid by HATU followed by de-protection to afford the corresponding amide **8h–m**. De-methylation of methoxy-substituted indazole **6** followed by displacement of various tosylates, after de-protection, yielded the corresponding ether-linked adducts **8f**, **8g**, **8q** and **8r**. To explore SAR on 1-phenyl substitution (R³) of indazole scaffold **12**, an efficient divergent synthesis was also developed as shown in Scheme 2. Suzuki coupling of commercially available 6-bromo-indazole **9** with 4-(4,4,5,5-tetramethyl-[1,3,2]dioxaborolan-2-yl)-3,6-dihydro-2H-pyridine-1-carboxylic acid tert-butyl ester gave indazole **10** in 75% yield. 3-Iodination of **10** with iodine and potassium hydroxide followed by palladium catalyzed methylthio-ether formation provided 3-methylthio-indazole **11** as the key intermediate in 45% yield. Thio-indazole **11** was then coupled with various phenyl-boronic acids by Cu(OAc)₂, after de-protection of the *N*-Boc group under acidic condition, to afford 3-(methylthio)-1-phenyl-1H-indazole **12** in moderate to good yield. 3-Methyl or 3-ethyl substituted indazoles **19** and **20** were synthesized according to the routes shown in Scheme 3.¹⁰ Ketones **13** and **14**, available through literature known methods,¹¹ were reacted with PhNHNH₂ under acid catalysis to give the corresponding hydrazones **15** and **16** in 75–100% yield. Intramolecular cyclizations occurred upon treatment of **15** and **16** with potassium carbonate to form indazole cores **17** and **18** in 45–60% yield. Compounds **19a–b** and **20a–j** were obtained through Suzuki, Buchwald or amide coupling procedures similar to the procedures described in Scheme 1.

The in vitro biological activity of all target compounds was evaluated in an enzyme assay that was developed to measure KHK-mediated conversion of D-fructose to fructose-1-P (F-1-P) using High Throughput Mass Spectroscopy (HTMS) as a means of product detection.¹² Our SAR studies initially focused on the pendant amino group (R²) of indazole **8**. Table 1 showed KHK enzyme activity of key compounds **8a–r**. In general, modifications at 6-position of indazole **8** could generate compounds with good activity provided that a basic amino group existed on the terminal position, with an exception of a terminal pyridinyl group noted in **8d**. After examining a range of substituents at 6-position of indazole scaffold **8**, we found that terminal piperidinyl or piperazinyl group (**8a** & **8b** in Table 1) provided good KHK enzyme activity (IC₅₀ of 0.33 and 0.56 μM, respectively). Compound **8c** bearing a tetrahydro-pyri-

Table 1
SAR on R² group of indazole **8**



8

ID	R ² (6-substitution)	KHK enzyme ^a IC ₅₀ (μM)
8a		0.33
8b		0.56
8c		0.08
8d		>10
8e		0.71
8f		0.71
8g		0.44
8h		0.33
8i		0.31
8j		0.59
8k		0.22
8l		0.68
8m		0.38
8n		0.67
8o		0.83
R ² (7-substitution)		
8p		11.5
8q		1.68
8r		0.24

^a High Throughput Mass Spectrometry (HTMS, BioTrove RapidFire™) format. IC₅₀ was determined in a 12 point dose–response curve under the established steady-state conditions of 200 μM fructose, 100 μM ATP and 2 nM KHK for 60 min at 25 °C.

dine (THP) substitution presented better potency with IC₅₀ of 0.08 μM. The steric hindrance of the piperazinyl ring was tolerated as illustrated by **8e** (IC₅₀, 0.71 μM) containing a bulky bicyclo-[2,2,1] ring system. We also modified the terminal basic amino group by introducing R² of variable length at the 6-position of indazole core. Compounds **8f** and **8g** bearing one- and two-atoms between the core and the piperidine showed comparable activities

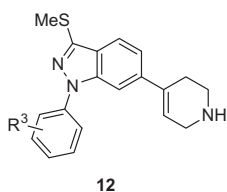
as **8a** with direct linkage. Varying the terminal basic amino group at either 3- or 4-position of piperidine ring (**8h** & **8i** in Table 1) resulted in equipotent compounds. The ring size was also well tolerated as illustrated by **8h**, **8j** and **8k** containing corresponding 6, 5 and 4 membered rings. We also observed that the length of the linkers at 6-position of indazole scaffold **8** was tolerated for KHK enzyme activity. Homologs of **8h** with longer pendant side chains were also tolerated for sub- μM activities, as shown in **8l** and **8m** (IC_{50} , 0.68 and 0.38 μM , respectively). This was further demonstrated by **8n** and **8o** bearing bicyclic pendant basic side chains (IC_{50} , 0.67 and 0.83 μM , respectively). SAR clearly indicated that there is room for modifications in this region for addressing physical properties of this scaffold. We next turned our attention to 7-position of indazole **8**. Analog **8p** with a 7-THP substitution displayed considerably lower KHK enzyme activity (IC_{50} , 11.5 μM) compared with the corresponding 6-THP counterpart **8c** (IC_{50} , 0.08 μM). Insertion of some linkers between the indazole core and the pendant amino side chain resulted in significant improvement in potency. For example, compound **8q** with a one atom oxy linker and **8r** with a two atom methyleneoxy linker dis-

played IC_{50} of 1.68 and 0.24 μM , respectively. Molecular modeling of 7-substituted indazoles suggested the terminal basic amino group of **8p** was too rigid to form a tight charge–charge interaction with carboxylate side-chain of β -clasp residue on the enzyme. Under this circumstance, installation of linkers on the side chain such as in **8r** could extend the side chain deeper into the ATP binding region to reach the key interaction with the Asp27B.

We then sought to investigate the substitution effect (R^3) of a 1-phenyl group on KHK enzyme activity. This sub-set of compounds (**12a–g**) all have a THP group at the 6-position of the indazole core. KHK enzyme activities were summarized in Table 2. Most compounds bearing small 3- or 4-substitution on the phenyl ring retained good potency whereas 4-nitro and 4-amino substituted phenyl analogs **12f** and **12g** tended to be less potent. Whilst fluoro analogs **12a** and **12b** were just slightly more potent than **8c** (IC_{50} , 0.042, 0.023 μM vs 0.08 μM), both compounds showed better metabolic stability in rat liver microsomes than **8c** (**12a**, 96% remaining at 10 min; **12b**, 105% remaining at 10 min; **8c**, 72% remaining at 10 min).

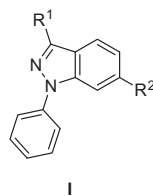
According to X-ray crystallographic information from library screening, replacement of 3-thiomethyl group on pyrazole **1** with other substitutions was not well tolerated. Thiomethyl groups are usually considered as a metabolically unfavorable functional group due to high tendency toward chemical or enzymatic oxidation. To complete SAR of the indazole series and to improve metabolic stability of indazole **2**, we replaced 3-thiomethyl with methoxy, methyl or ethyl groups (Table 3). Not surprisingly, 3-methoxy and 3-methyl substituted analogs showed reduced

Table 2
SAR on R^3 group of indazole **12**



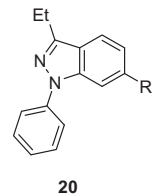
ID	R^3	KHK enzyme IC_{50} (μM)
8c	H	0.080
12a	3-F	0.042
12b	4-F	0.023
12c	3-Me	0.034
12d	4-Me	0.04
12e	4-OMe	0.087
12f	4-NO ₂	0.48
12g	4-NH ₂	0.16

Table 3
SAR on R^1 and R^2 groups of indazole **1**



ID	R^1	R^2	KHK enzyme IC_{50} (μM)
8b	SMe	—N(CH ₂) ₆ NH	0.56
8n	SMe	—N(CH ₂) ₆ N(CH ₂) ₆ NH	0.67
19a	Me	—N(CH ₂) ₆ NH	1.28
19b	Me	—N(CH ₂) ₆ N(CH ₂) ₆ NH	3.20
7a	OMe	—N(CH ₂) ₆ NH	1.38
20a	Et	—N(CH ₂) ₆ NH	0.57
20b	Et	—N(CH ₂) ₆ N(CH ₂) ₆ NH	0.56

Table 4
SAR on R^2 group of indazole **20**



ID	R^2	KHK enzyme IC_{50} (μM)
20a	—N(CH ₂) ₆ NH	0.57
20b	—N(CH ₂) ₆ N(CH ₂) ₆ NH	0.56
20c	—N(CH ₂) ₆ NH (Me)	0.86
20d	—N(CH ₂) ₆ N-Me	4.52
20e	—N(CH ₂) ₆ N-Et	11.5
20f	—N(CH ₂) ₆ NH (indole)	0.59
20g	—N(CH ₂) ₆ NH (pyrrolidine)	0.92
20h	—N(CH ₂) ₆ NH (pyridine)	3.52
20i	—N(CH ₂) ₆ NH (phenyl)	9.80
20j	—NH-C(=O)-C ₆ H ₄ -NH-C(=O)-NH ₂	0.68
20k	—NH-C(=O)-C ₆ H ₃ (N)-NH ₂	0.94

potency compared with the corresponding 3-thiomethylated indazoles. Compounds **7a**, **19a** and **19b** only showed low μM KHK enzyme activity. In contrast to the observation from library screening, some 3-ethylated analogs were equipotent to their corresponding 3-thiomethyl indazoles. For example, replacement of thiomethyl in **8b** (IC_{50} of 0.56 μM) and **8n** (IC_{50} of 0.67 μM) with ethyl gave **20a** and **20b** with IC_{50} of 0.57 and 0.56 μM , respectively, which demonstrated that the ethyl group was an effective bioisostere for the thiomethyl group.

We then turned our attention on optimization of the 3-Et-indazole on R^2 substitution (Table 4). Both steric effects and the basicity of the terminal amine play important roles for efficient interaction with the acidic ASP27B. While **20c** bearing a α methyl group to the terminal amine showed a slight potency drop compared with **20a** (IC_{50} of **20a**, 0.57 μM vs **20c**, 0.86 μM), methylation of the secondary amino group of **20a** resulted in more than seven fold decrease in potency in **20c** (IC_{50} , 4.52 μM). Ethylation led to even more activity loss as shown in **20d** (IC_{50} , 11.5 μM). Pyridinyl analog **20h** bearing a relatively weaker basic group displayed weaker KHK enzyme activity (IC_{50} , 3.52 μM) as compared with **20b** and **20g** (IC_{50} , 0.56 and 0.92 μM), although the rigidity of the pyridine ring could be another factor on its reduced activity. It was not surprising to observe that **20f** bearing a 5,5-fused amino substitution

at 6-position was well tolerated for sub- μM KHK enzyme activity (IC_{50} , 0.59 μM). According to SAR findings in Table 1, it is further suggested that the size and length of the R^2 group were well tolerated in this region. While the basic amino group was crucial for KHK enzyme activity for indazoles **20**, a well positioned linker had great impact for the favorable ionic interaction. Replacement of the more flexible piperidine ring of **20b** with the rigid phenyl ring of **20i** reduced activity almost twenty fold (IC_{50} , 9.80 μM), which indicated the planarity of the phenyl ring directed the terminal basic amino group to an unfavorable distance from Asp27B. It is interesting to observe that compounds bearing terminal basic groups other than secondary amines could still maintain decent potency. For example, compound **20j** with a terminal amidate and **20k** with a terminal imidazole exhibited good KHK enzyme activity with IC_{50} of 0.68 and 0.94 μM , respectively.

We also incorporated structurally similar scaffolds to expand the scope around the indazole template. To this end, isomeric indazole **21**, pyrazolo-pyrimidinone **22** and imidazopyridine **23** were synthesized and their KHK enzyme activities were evaluated as shown in Figure 2. Although these isosteric heterocyclic 6,5-fused core systems showed striking structural similarity for maintaining H-bonding between 2-nitrogen atom of the five membered heterocycle with the conserved water, they may provide very different physicochemical property. The data indicated that compound **21** maintains KHK enzyme activity (IC_{50} , 1.28 μM), while compound **22** with pyrazolo-pyrimidinone skeleton lost five fold activity (IC_{50} , 6.10 μM) compared to indazole **19a**. The imidazopyridine core shown in **23** was not tolerated at all.

The X-ray crystal structure of **20f** bound to the active site of KHK revealed that **20f** binds in the ATP site following the same fashion as FBDD hit **1** (Fig. 3).¹³ The 2-nitrogen of indazole core formed key H-bonding to the conserved water. The 3-ethyl group of indazole **20f** projected toward the aromatic side chain of Phe260 in the pocket to form a hydrophobic interaction. The flat indazole core bound to the lipophilic residues from both the α/β and β -sheet domains of KHK at the narrow central region of

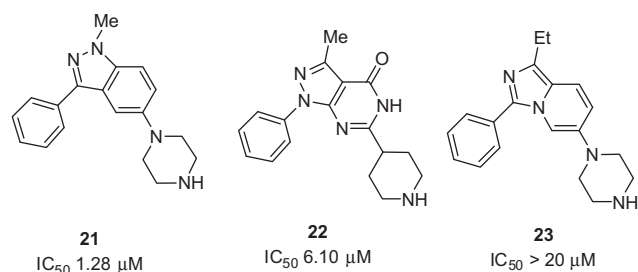


Figure 2.

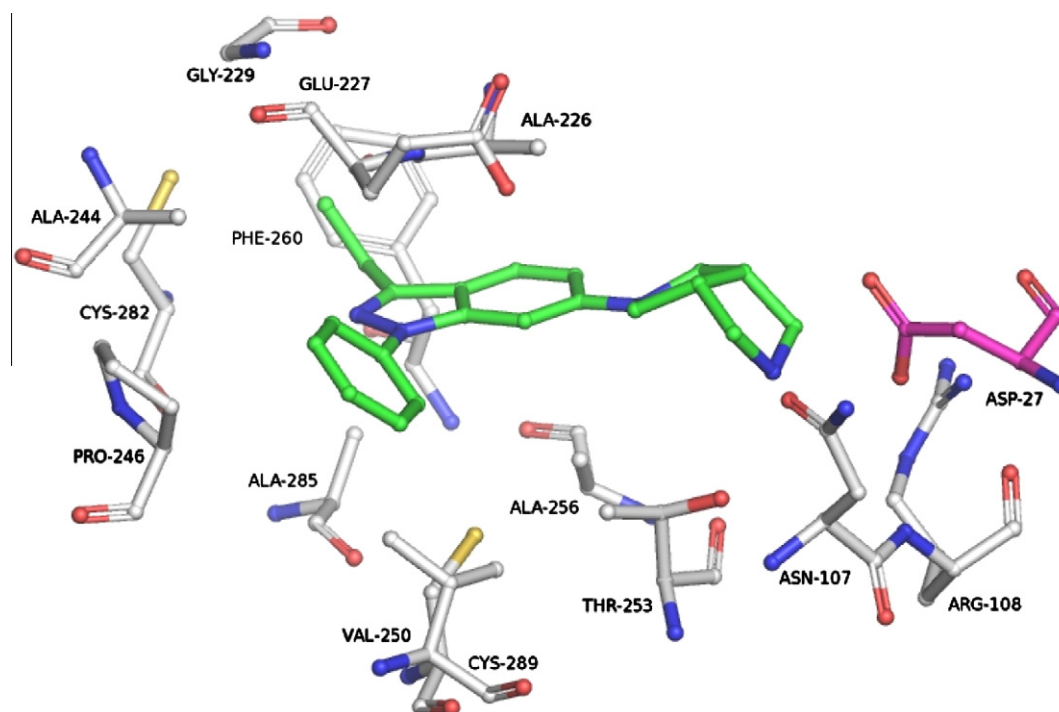


Figure 3. X-ray co-crystal structure of **20f** bound to the active site of KHK.

Table 5
In vivo rat DMPK profiles of selected indazoles^a

Cpd	PO ^a	t _{1/2} (h)	C _{max} (ng/μL)	AUC _{last} (h * ng/μL)	IV ^b	V _{ss} (L/kg)	CL (mL/min/kg)	F (%)
20f	10 mpk	3.41	619	5679	2 mpk	7.81	28.9	98.8
20g	10 mpk	19.6	399	4887	2 mpk	13.9	21.2	72.4

^a PO (10 mg/kg) in 0.5% methocel.

^b IV (2 mg/kg) in 20% HPBCD.

the active site. Additionally, a small hydrophobic pocket was formed between the 1-substituted phenyl group and three sequential proline residues, Pro246–248. The tight binding mode of the central region of the active site allowed the carboxylate side-chain of β-clasp residue Asp27B to pack next to the fragment. The [3.3.0] bicyclic amino side chain attached to the indazole core in the closed catalytic site and the terminal amino group was engaged in both ionic interactions with the carboxylate residue of Asp27B and hydrogen bonding with Asn107.

Selected compounds according to their eADME profiles were evaluated in a 24 h rat pharmacokinetic study at an oral dose of 10 mg/kg and iv dose of 2 mg/kg (Table 5). Compounds **20f** and **20g** demonstrated good oral bioavailability (98.8% and 72.4%) and good oral exposure in plasma (AUC_{last} = 5679 and 4887 ng h/mL). Both compounds had moderate clearance (28.9 and 21.2 mL/min kg) and volume of distribution at steady state (V_{ss} = 7.81 and 13.9 L/kg) within our target range. In addition, several compounds from this scaffold were submitted to the Cerep 'Comprehensive Pharmacological Profile' panel, including more than 100 biological targets (GPCRs, ion channels, transporters and enzymes). All compounds showed clean selectivity profiles at 10 μM in the full panel.¹⁴

In summary, a lead generation process has been conducted for discovering novel indazoles as KHK inhibitors. Optimization of an indazole series according to KHK enzyme activity produced compounds with nanomolar KHK enzyme activity. Furthermore, the PK profiles of lead compounds proved to be acceptable with moderate blood clearance, high volume of distribution, and high oral bioavailability. The lead compounds from this series therefore deserve to be further explored in vivo to exploit the therapeutic potential as KHK inhibitors for metabolic diseases.

Acknowledgments

The authors would like to thank ADME/PK, Analytical Research and Lead Generation Biology teams at Johnson & Johnson Pharmaceutical Research and Development for service support. The authors would also like to thank the staff at IMCA-CAT for their assistance during X-ray data collection. The use of the IMCA-CAT beam lines 17-ID and 17-BM at the Advanced Photon Source was supported by the companies of the Industrial Macromolecular Crystallography Association through a contract with Hauptman–Woodward Medical Research Institute. Use of the Advanced Photon Source was supported by the US Department of Energy, Office of Science, Office of Basic Energy Sciences, under Contract No. W-31-109-Eng-38.

References and notes

- Rauschel, F. M.; Cleland, W. W. *Biochemistry* **1977**, *16*, 2169.
- Gross, L. S.; Li, L.; Ford, E. S.; Liu, S. *Am. J. Clin. Nutr.* **2004**, *79*, 774.
- Basciano, H.; Federico, L.; Adeli, K. *Nutr. Metab.* **2005**, *2*, 5.
- Maryanoff, B. E.; O'Neill, J. C.; McComsey, D. F.; Yabut, S. C.; Luci, D. K.; Jordan, A. D.; Masucci, J. A.; Jones, W. J.; Abad, M. C.; Gibbs, A. C.; Petrounia, I. *ACS Med. Chem. Lett.* ACS ASAP.
- Gibbs, A. C.; Abad, M. C.; Zhang, X.; Tounge, B. A.; Lewandowski, F. A.; Struble, G. T.; Sun, W.; Sui, Z.; Kuo, L. C. *J. Med. Chem.* **2010**, *53*, 7979.
- Warr, W. A. *J. Comput. Aided Mol. Des.* **2009**, *23*, 453.
- Congreve, W.; Chessari, G.; Tisi, D.; Woodhead, A. J. *J. Med. Chem.* **2008**, *51*, 3661.
- Orita, M.; Warizaya, M.; Amano, Y.; Ohno, K.; Niimi, T. *Expert Opin. Drug Discov.* **2009**, *4*, 1125.
- De Kloe, G. E.; Bailey, D.; Leurs, R.; de Esch, I. J. P. *Drug Discovery Today* **2009**, *14*, 630.
- 3-Ethyl-6-(hexahydropyrrolo[3,4-c]pyrrol-2(1H)-yl)-1-phenyl-1H-indazolehydrochloride (**20f**): Into a 1000-mL round-bottom flask, was placed a solution of 1-(4-bromo-2-fluorophenyl)propan-1-one (32 g, 138.53 mmol, 1.00 equiv) in ethanol (300 mL), 1-phenylhydrazine (15.0 g, 138.89 mmol, 1.00 equiv), TSA-H₂O (1.32 g, 6.95 mmol, 0.05 equiv). The resulting solution was heated to reflux for 1 h in an oil bath. The resulting mixture was concentrated under vacuum to yield 1-(1-(4-bromo-2-fluorophenyl)propylidene)-2-phenylhydrazine as a yellow solid (44.3 g, yield: 99%). MS: 322 (MH⁺). Into a 1000-mL 3-necked round-bottom flask, was placed a solution of 1-(1-(4-bromo-2-fluorophenyl)propylidene)-2-phenylhydrazine (44.3 g, 138.01 mmol, 1.00 equiv) in *N,N*-dimethylformamide (400 mL), potassium carbonate (83 g, 601.45 mmol, 4.40 equiv). The resulting solution was stirred for 2 days at 100 °C in an oil bath. The resulting mixture was concentrated under vacuum. The resulting solution was diluted with water (500 mL). The resulting solution was extracted with ethyl acetate (2 × 300 mL) and the organic layers combined. The resulting mixture was washed with water (2 × 300 mL) and brine (1 × 300 mL). The resulting mixture was dried over anhydrous sodium sulfate and concentrated under vacuum. The residue was applied onto a silica gel column with ethyl acetate/petroleum ether (1:50) to yield 6-bromo-3-ethyl-1-phenyl-1H-indazole as a yellow solid (20.8 g, yield: 50%). MS (*m/z*): 301 [M+H]⁺; ¹H NMR (400 MHz, CDCl₃, ppm): δ 1.42–1.46 (3H, t), 3.01–3.07 (2H, dd), 7.25–7.86 (8H, m). Into a 100-mL 3-necked round-bottom flask purged and maintained with an inert atmosphere of nitrogen, was placed a solution of 6-bromo-3-ethyl-1-phenyl-1H-indazole (300 mg, 1.00 mmol, 1.00 equiv) in toluene (30 mL), *tert*-butyl hexahydropyrrolo[3,4-c]pyrrole-2(1H)-carboxylate (212 mg, 1.00 mmol, 1.00 equiv), Pd(OAc)₂ (2.24 mg, 0.01 mmol, 0.01 equiv), Cs₂CO₃ (482 mg, 2.50 mmol, 2.50 equiv), BINAP (18.7 mg, 0.03 mmol, 0.03 equiv). The resulting solution was heated to reflux overnight in an oil bath. The resulting mixture was concentrated under vacuum. The residue was applied onto a silica gel column with dichloromethane/methanol (100:1). The residue was dissolved in hydrogen chloride/MeOH (50 mL) and then stirred for 2 h at room temperature. The resulting mixture was concentrated under vacuum and the residue by re-crystallization from diethyl ether (50 mL). The solids were collected by filtration, was dried in an oven under reduced pressure to yield 3-ethyl-6-(hexahydropyrrolo[3,4-c]pyrrol-2(1H)-yl)-1-phenyl-1H-indazolehydrochloride as a white solid (170 mg, yield: 46%). MS (*m/z*): 333 [M-HCl+H]⁺; ¹H NMR (400 MHz, DMSO, ppm): δ 1.33 (3H, t), 2.92 (2H, q), 3.08 (4H, m), 3.42 (6H, m), 3.89 (3H, s), 6.71–7.72 (8H, m), 9.35 (2H, s).
- Wang, C. H.; Feng, T. C.; Christensen, B. E. *J. Am. Chem. Soc.* **1950**, *72*, 4887.
- An enzymatic assay was developed to measure KHK-mediated conversion of D-fructose to fructose-1-P (F-1-P) using High Throughput Mass Spectroscopy (HTMS) as a means of product detection. This assay served as a primary screen to evaluate the ability to inhibit KHK enzyme activity and it has been adapted to high throughput mass spectrometry (HTMS, BioTrove RapidFire™) format for higher throughput. The compounds to be tested were dosed in 12-points. Inhibition of the fragment, IC₅₀, was determined in a dose–response curve under the established steady-state conditions of 200 μM fructose, 100 μM ATP and 2 nM KHK for 60 min at 25 °C. The assay was carried out in 384-well plate format.
- The atomic coordinate and structure factor for the KHK complexes with compound **20f** have been deposited in the Protein Data Bank under accession code (pdbid: 3NBW).
- A representative compound **20b** in Cerep panel: only hit, Na channel, 61% at 10 μM.